Physics – Uspekhi **48** (2) 151 – 166 (2005)

REVIEWS OF TOPICAL PROBLEMS PACS numbers: **02.50. – r**, **05.45. – a**, **47.52. + j**

Statistical properties of dynamical chaos

V S Anishchenko, T E Vadivasova, G A Okrokvertskhov, G I Strelkova

DOI: 10.1070/PU2005v048n02ABEH002070

Contents

Abstract. Statistical descriptions of dynamical chaos and investigations of noise effects on chaotic oscillation regimes are reviewed. Nearly hyperbolic and nonhyperbolic chaotic attractors are studied. An illustration of the technique of diagnosing the attractor type in numerical simulations is given. Regularities in relaxation to the invariant probability distribution are analyzed for various types of attractors. Spectral-correlative properties of chaotic oscillations are investigated. Decay laws for the autocorrelation functions and the shapes of the power spectra are found, along with their relationship to the Lyapunov exponents, diffusion of the instantaneous phase, and the intensity of external noise. The mechanism of the onset of chaos and its relationship to the characteristics of the spiral attractors are demonstrated for inhomogeneous media that can be modeled by the Ginzburg – Landau equation. Numerical data are compared with experimental results.

1. Introduction

Dynamical chaos, as a random process, requires a statistical description. As chaotic systems are studied in laboratory experiments or simulated numerically, some probabilistic characteristics are normally calculated or measured, such as the stationary probability distribution over the attractor, correlation functions, power spectra, etc. Chaotic oscillations, which can be mathematically represented by chaotic attractors of various types, differ in their statistical properties and their sensibility to the influence of noise.

From the standpoint of rigorous theory, hyperbolic chaos is frequently said to be the 'ideal' chaos. Its structure is topologically homogeneous and stable against disturbances [1 – 4]. However, as a rule, the strange chaotic attractors of dynamical systems do not behave as structurally stable hyperbolic systems. Nearly hyperbolic (quasi-hyperbolic) attractors include unstable orbits of the separatrix-loop type. The generation and disappearance of such orbits do not affect the characteristics of chaos such as the phase portrait of the attractor, the power spectrum, the Lyapunov exponents, etc. Dynamical systems in chaotic regimes can be characterized by an invariant measure that is independent of the initial distribution and completely specifies the statistical properties of the attractor. The existence of an invariant measure has been proven theoretically for structurally stable hyperbolic and quasi-hyperbolic systems [5 – 10].

However, most chaotic attractors that have been studied numerically and/or experimentally are not hyperbolic [11 – 13]. The problem of the existence of an invariant measure on a nonhyperbolic chaotic attractor encounters serious difficulties because a stationary probability distribution independent of the initial distribution cannot be introduced in general. The nonhyperbolic attractor is the maximal attractor of the dynamical system; it includes a countable set of regular and chaotic attracting subsets [11, 12]. Therefore, one can consider the invariant measure of a nonhyperbolic attractor only if the influence of external noise is present [14]. As a rule, nonhyperbolic attractors change their properties dramatically under the action of noise [15 – 18], whereas hyperbolic and quasi-hyperbolic attractors are stable against noise disturbances [15, 16, 19, 20],

The statistical description of noise-affected nonhyperbolic chaotic attractors is an important problem of the

V S Anishchenko, T E Vadivasova, G A Okrokvertskhov, G I Strelkova
Department of Physics, Institute of Nonlinear Dynamics,
Saratov State University,
ul. Astrakhanskaya 83, 410012 Saratov, Russian Federation
Tel. (7-8452) 51 57 38. Fax (7-8452) 51 45 49
E-mail: wadim@chaos.ssu.runnet.ru

Received 17 September 2004
Uspekhi Fizicheskikh Nauk **175** (2) 163 – 179 (2005)
Translated by A V Getling; edited by A M Semikhatov

theory of dynamical chaos that still remains unresolved. Among other things, the relaxation time to a stationary distribution should be investigated. A number of fundamental questions that have not yet been clearly answered arise. What is the actual relaxation time to a stationary distribution? What are the factors controlling this time? What characteristics could be used to quantitatively estimate the relaxation time for the stationary measure? How do the noise statistics and noise intensity affect the law of relaxation to the stationary distribution? Is the relaxation process related to the dynamics of the system? These questions were partly answered in Refs [21, 22] by means of computer simulations.

The process of relaxation to a stationary distribution can be described by Fokker – Planck-type or Frobenius – Perron-type evolutionary equations. The eigenvalues and eigenfunctions of the evolution operator specify the relaxation process and the characteristics of mixing, which are linked to the relaxation to the invariant probability measure. However, if the dimension of the dynamical system is high ($N \geqslant 3$), the Fokker – Planck and Frobenius – Perron equations are virtually unsolvable, even in a numerical form. For this reason, the studies described in Refs [21, 22] used the technique of stochastic differential equations.

By definition, chaotic dynamics implies mixing and, therefore, a positive Kolmogorov entropy. As a result of mixing, autocorrelation functions decrease to zero (correlation splitting). States of the system separated by a sufficiently long time interval become statistically independent [6, 8, 23 – 25]. It is important to note that any system with mixing is ergodic. The temporal splitting of correlations in chaotic dynamical systems is related to the exponential instability of chaotic trajectories and to the system's property of generating a positive Kolmogorov entropy [6, 8, 23 – 27]. Although the correlation properties of chaotic processes are very important, they have not yet been adequately explored. It is commonly assumed that the autocorrelation functions of chaotic systems decay exponentially at a rate determined by the Kolmogorov entropy [23]. It is then assumed that the Kolmogorov entropy H_K is bounded from above by the sum of positive Lyapunov exponents [8, 27, 28]. Regrettably, this estimate proves to be wrong in the general case of hyperbolic systems.

It has been proven for certain classes of discrete mappings with mixing (expanding mappings with a continuous measure and the Anosov diffeomorphism) that the time decrease in the correlations is bounded from above by an exponential function [9, 29 – 31]. Various estimates have been obtained for the rate of this exponential decay, which are not always related to the Lyapunov exponents [21, 32 – 34]. As regards systems with continuous time, no theoretical estimates for the rate of correlation splitting are available as yet [35].

Experimental studies of some particular chaotic systems testify to a complex behavior of the correlation functions, which is controlled not only by the positive Lyapunov exponents but also by the properties of the chaotic dynamics of the system [21, 32, 34, 36]. It is important to reveal specific parameters of the chaotic dynamics that are responsible for the decay rate of the autocorrelations and for the spectral-line width of the fundamental frequency of the chaotic attractor. Our aim here is to survey our results [21, 22, 37 – 39] obtained recently in studying classical systems with nonhyperbolic and quasi-hyperbolic attractors [40 – 43]. These results include a technique for diagnosing nonhyperbolic chaos, noise effects on nonhyperbolic attractors, some probabilistic aspects of chaotic dynamics (such as the features of the relaxation to the stationary probability distribution and the mixing rate), and a spectral-correlative analysis of various types of chaotic oscillation regimes. Particular attention is given in our review to the influence of external noise on the statistical properties of chaos.

2. Diagnosis of hyperbolicity in chaotic systems

Strange attractors in finite-dimensional systems can be divided into three basic classes: structurally stable (robust) hyperbolic, almost hyperbolic (quasi-hyperbolic), and nonhyperbolic [11 – 13]. The property of robust hyperbolicity of a chaotic attractor implies that all its trajectories are of the same saddle type, and their stable and unstable manifolds are everywhere transverse, i.e., the structure of the hyperbolic attractor is homogeneous at any point of the attractor. Furthermore, small perturbations of the parameters of the system preserve these properties. But structurally stable hyperbolic attractors are rather typical of idealized objects such as the Smale – Williams solenoid [44] or the Plykin attractor [45]. The existence of a robust hyperbolic attractor has not been proven for dynamical systems specified by differential equations or discrete mappings. Nevertheless, several examples of almost hyperbolic attractors are known for such systems. These are the Lorenz attractor [46] and the Shimizu – Morioka attractor [47] in flow systems and the Lozi attractor [48] and the Belykh attractor [49] in discrete mappings. Singular phase trajectories are characteristic of these systems. For example, the Lorenz attractor is characterized by the presence of a set of separatrix loops of the saddle-point-type equilibrium state, whereas the Lozi attractor includes nonrobust homoclinic curves without tangencies between stable and unstable manifolds. However, these peculiar trajectories do not generate stable motions, and the quasi-hyperbolic and hyperbolic attractors are similar from the standpoint of numerical simulation.

Most chaotic attractors of dynamical systems are nonhyperbolic [11 – 13]. Nonhyperbolic attractors include chaotic limiting sets and stable periodic orbits that, as a rule, are difficult to detect in numerical simulations, because they have extremely small attracting basins. If the whole collection of properties is considered, nonhyperbolic attractors differ substantially from hyperbolic ones [13, 50, 51]. Therefore, the diagnosis of the attractor type is of paramount importance for the analysis of nonlinear systems in both the theoretical and practical contexts [17, 52 – 57].

The direct technique of determining the conditions of hyperbolicity includes the calculation of the angles ϕ between the stable and unstable manifolds along a phase trajectory. A numerical procedure of computing these angles was proposed by Lai et al. [58] as a tool for diagnosing the hyperbolicity of chaotic saddle points in two-dimensional systems. This technique consists of transforming an arbitrary vector by the evolution operator in both direct and reverse time, which makes it possible to find the angle between the directions of stability and instability for various points of chaotic sets.

Manifolds are one-dimensional in two-dimensional systems, and hence diagnosing the effect of homoclinic tangency does not present major difficulties. The problem is more complex for three-dimensional systems, because the manifolds are two-dimensional in this case. We have suggested a method for diagnosing hyperbolicity in three-dimensional

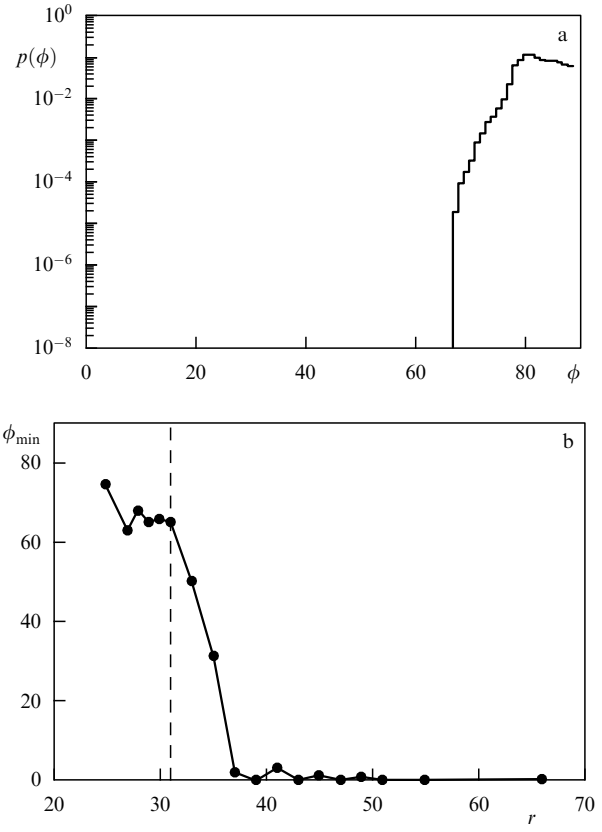

Figure 1. Calculation results for Lorenz system (1) at $\sigma = 10$ and $\beta = 8/3$: (a) probability distribution of angles for the Lorenz attractor at $r = 27$; (b) the minimum angle $\phi_{\min}$ as a function of the parameter r. The vertical line marks the theoretically determined onset of the transition from the Lorenz attractor to nonhyperbolic attractors.

differential systems [59]. It was found that systems such as the Rössler system, the Chua circuit [60], and the Anishchenko–Astakhov oscillator are typically nonhyperbolic, i.e., structurally unstable systems [11]. The Lorenz system can be considered an exception. The Lorenz attractor is almost hyperbolic in a certain parameter range. The stable and unstable manifolds of the attractor trajectories intersect transversely [59]. However, as the parameters are varied, the Lorenz system exhibits a bifurcational transition to a nonhyperbolic attractor [61]. Figure 1a shows the probability distribution of angles $p(\phi)$ for the Lorenz attractor in the system [41]

$$\dot{x} = -\sigma(x - y), \quad \dot{y} = rx - y - xz, \quad \dot{z} = -\beta z + xy. \quad (1)$$

It can be seen from the upper graph that the probability of homoclinic contact is exactly zero $[p(\phi) = 0]$. As the region where the Lorenz attractor exists recedes, the effect of homoclinic contact emerges (Fig. 1b). Evidently, the angle between the manifolds can vanish at $r \geqslant 38$ (Fig. 1b). This effect largely accounts for the properties of nonhyperbolic chaos, which are considered in subsequent sections of our article.

3. Chaos in the presence of noise

Nonlinear stochastic problems are of fundamental and practical importance. Two basic approaches to the analysis of stochastic systems are known [62–65]. The first is based on solving *stochastic equations* and is called the *Langevin method*. Any particular solution of stochastic equations, even for the same initial state, generates a new realization of the random process. This method allows obtaining an ensemble of a large number of realizations and finding a statistical characterization of the process. Averaging can be done over one, sufficiently long, realization, because the chaotic process is ergodic. The second approach consists in solving the *evolutionary equations for the probability measure*, such as the Chapman–Kolmogorov equation, the kinetic equation, or the Fokker–Planck equation. This requires that the random process in the system be at least Markovian, which poses some constraints on the noise sources. For the process to be Markovian, random actions must be independent. In this case, the Chapman–Kolmogorov equation is valid. If the noise is Gaussian, the process is diffusive, and the probability density obeys the Fokker–Planck equation. If the noise sources satisfy the corresponding requirements, the method of stochastic equations and the method of evolutionary equations must yield equivalent results [62–64, 66].

The problem of statistical characterization of dynamical chaos and the role of fluctuations in chaotic systems is of particular interest [6, 7, 19, 42, 66–70]. For systems with hyperbolic-type chaotic dynamics, statistical description is possible even in purely deterministic cases, i.e., in the absence of noise [6, 7, 19, 70]. This means that the stationary solution of the evolutionary equation for the probability density allows the existence of the limit as $D \to 0$, where D is the noise intensity; therefore, a solution for the probability measure can be obtained even in a purely deterministic case. As shown in Refs [6, 19], small fluctuations ($D \ll 1$) in hyperbolic systems give rise to small variations in the structure of the probability measure. From this standpoint, so-called quasi-hyperbolic (almost hyperbolic) attractors, such as the Lozi attractor and the Lorenz attractor [11, 12], do not virtually differ from hyperbolic attractors. This is because neither quasi-hyperbolic nor hyperbolic attractors contain stable periodic orbits. A rigorous proof of the existence of a probability measure in the Lorenz attractor in the absence of noise was given in Ref. [7].

The effects of noise are important for nonhyperbolic systems. As shown in Ref. [16], the mean distance between an orbit with noise and a nonhyperbolic attractor without noise is much larger than in the hyperbolic case and depends on the informational dimension of the attractor. It is well known that noise can induce various phase transitions in systems with nonhyperbolic attractors [42, 43, 71, 72]. As sources of Gaussian noise are added to the system, the attraction basins of the coexisting attractors merge. This results in relaxation to a stationary probability density, which is independent of the initial state [14]. A statistical description of nonhyperbolic chaos encounters fundamental difficulties. Strictly speaking, a stationary probability measure independent of the initial distribution does not exist in nonhyperbolic chaotic attractors without noise. The continuum limit as $D \to 0$ cannot be implemented in this case [14]. Moreover, probabilistic characteristics of nonhyperbolic chaos are highly sensitive even to tiny variations in the parameters of the system [13, 42, 59, 73]. Thus, the existence of a stationary probability measure in a nonhyperbolic attractor is only possible if the system is affected by noise.

4. Relaxation to the stationary probability distribution for chaotic attractors in the presence of noise

4.1 Models and numerical techniques

We now consider the chaotic attractors of the well-known systems such as the Rössler oscillator [40]

$$\dot{x} = -y - z + \sqrt{2D}\,\xi(t)\,, \quad \dot{y} = x + ay\,, \quad \dot{z} = b - z(m - x) \tag{2}$$

and the noise-affected Lorenz system (1) [41]

$$\begin{aligned} \dot{x} &= -\sigma(x - y) + \sqrt{2D}\,\xi(t)\,, \\ \dot{y} &= rx - y - xz\,, \\ \dot{z} &= -\beta z + xy\,. \end{aligned} \tag{3}$$

In both models, $\xi(t)$ is the source of Gaussian white noise with the mean value $\langle \xi(t) \rangle \equiv 0$ and correlation $\langle \xi(t)\xi(t+\tau) \rangle \equiv \delta(\tau)$, where $\delta(\tau)$ is the Dirac delta function. The parameter D denotes the noise intensity. For the Rössler system, we fix the parameters $a = 0.2$ and $b = 0.2$, varying the parameter m within the range $[4.25, 13]$. For the Lorenz system, we choose two different regimes — a quasi-hyperbolic attractor ($\sigma = 10$, $\beta = 8/3$, and $r = 28$) and a nonhyperbolic attractor ($\sigma = 10$, $\beta = 8/3$, and $r = 210$).

The chaotic attractors of systems (2) and (3) have been studied in detail and are classical examples of quasi-hyperbolic and nonhyperbolic chaos, respectively [43, 74]. Thus, the results obtained for Eqns (2) and (3) can be generalized to a broad class of dynamical systems.

To study the processes of relaxation to a stationary distribution in these systems, we analyze the time evolution of a collection of points initially located in a cube of a small size δ around an arbitrary point of a trajectory that belongs to the attractor of the system. We choose the size of this cube to be $\delta = 0.09$ and fill the cube uniformly with points whose number is $n = 9000$. In due course, they spread over the entire attractor. To characterize the convergence to a stationary distribution, we trace the time evolution of the set of points and calculate the ensemble average

$$\bar{x}(t) = \int_W p(x,t)\,x\,\mathrm{d}x = \frac{1}{n}\sum_{i=1}^{n} x_i(t)\,, \tag{4}$$

where x is one of the dynamical variables of the system and $p(x,t)$ is the probability density of the variable x at time t, which corresponds to the initial distribution. We introduce the function

$$\gamma(t_k) = \left|\bar{x}_m(t_{k+1}) - \bar{x}_m(t_k)\right|, \tag{5}$$

where $\bar{x}_m(t_k)$ and $\bar{x}_m(t_{k+1})$ are successive extrema of $\bar{x}(t)$. The function $\gamma(t_k)$ characterizes the amplitude of fluctuations in the mean of $\bar{x}_m(t)$. The successive time instants t_k and t_{k+1} in (5) correspond to the extrema of $\bar{x}$. The temporal behavior of $\gamma(t_k)$ gives an idea of the regularities and rate of relaxation to the probability measure in the attractor. We calculated the highest Lyapunov exponent λ_1 of a chaotic trajectory on the attractor and the normalized autocorrelation function (ACF) of the well-established oscillations $x(t)$:

$$\Psi(\tau) = \frac{\psi(\tau)}{\psi(0)}\,, \quad \psi(\tau) = \big\langle x(t)x(t+\tau) \big\rangle - \big\langle x(t) \big\rangle \big\langle x(t+\tau) \big\rangle\,. \tag{6}$$

Here, the angular brackets $\langle \ldots \rangle$ denote time averaging.

Instead of $\gamma(t_k)$ and $\Psi(\tau)$, we plot their respective envelopes $\gamma_0(t_k)$ and $\Psi_0(\tau)$, to make the figures more informative and visual.

4.2 Relaxation to the stationary distribution in the Rössler system. Effects of noise on the mixing rate

The nonhyperbolic chaotic attractor that appears in the Rössler system (2) at fixed $a = b = 0.2$ and at m values within the interval $[4.25, 8.5]$ is a well-known example of a spiral (or phase-coherent) attractor. The phase trajectory in a spiral attractor winds around one or several saddle foci. The ACF is oscillatory, and narrow-band peaks stand out in its power spectrum; they correspond to the mean winding frequency and its harmonics and subharmonics [43, 75–77].

As the parameter m is increased, the attractor of system (2) changes qualitatively. An incoherent attractor arises within the interval $8.5 < m \leqslant 13$, which is called a funnel attractor [42, 76]. The phase trajectories behave in a more complex way in it. As a result, the ACF of the funnel attractor decays much more rapidly than in the case of spiral chaos, and the power spectrum does not contain pronounced peaks.

Calculations carried out for $m \in [4.25, 7.5]$ (spiral chaos) and for $m \in [8.5, 13]$ (funnel chaos) without including noise suggest that an invariant probability measure exists at these parameter values.[1] Qualitatively, all effects observed in system (2) for each attractor type are preserved as the parameter m is varied.

Figure 2 shows a typical behavior of the function $\gamma_0(t)$ for the spiral and the funnel attractor of system (2). It has been found that noise strongly affects the mixing rate in the spiral-attractor regime. The relaxation time considerably decreases with the increase in the noise intensity (Fig. 2a). The situation is radically different in the case of the funnel attractor. Incoherent chaos is virtually insensitive to noise influences. The behavior of $\gamma_0(t)$ does not change substantially as noise is added (Fig. 2b). Numerical simulations show that the correlation times are also quite different for these two chaotic regimes: in the absence of noise effects, they differ by two orders of magnitude. For spiral chaos, the correlation time is considerably shorter in the presence of noise (Fig. 3a), while the ACF for the funnel attractor in the deterministic case virtually coincides with the ACF in the presence of chaos (Fig. 3b). Therefore, nonhyperbolic incoherent chaos exhibits some properties of hyperbolic chaos, i.e., as Sinaĭ noted [6], 'dynamical stochasticity' proves to be stronger than the stochasticity enforced from outside. This interesting result requires a more detailed consideration.

We also note another result. It has been found that a positive Lyapunov exponent is weakly sensitive to fluctuation effects for both spiral and funnel chaos (Fig. 4) and slightly decreases as noise is intensified. The correlation time can, however, vary significantly under the influence of noise in this case. Thus, mixing in the regime of spiral chaos is determined

[1] Stable trajectories have vanishingly small basins of attraction and do not manifest themselves, because the accuracy of computations is finite.

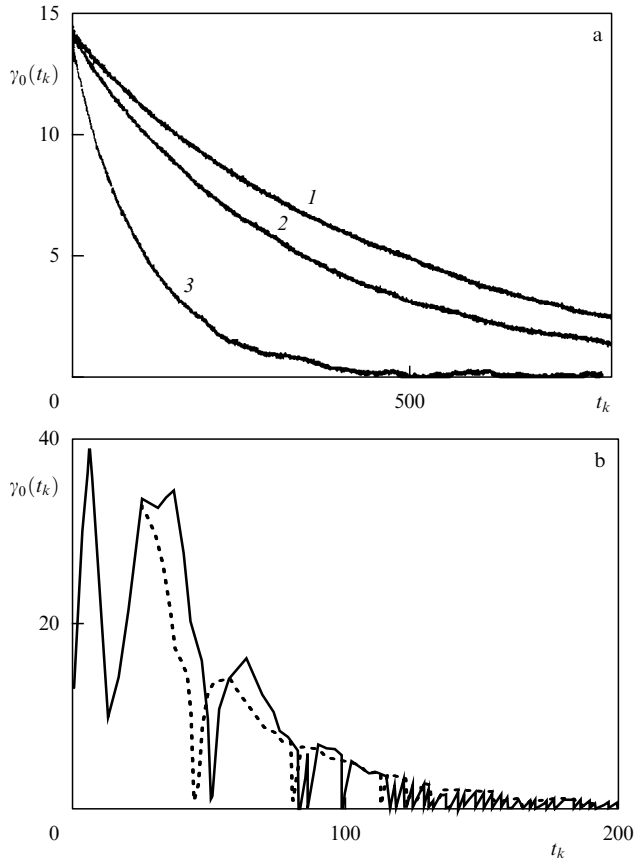

Figure 2. Behavior of the function $\gamma_0(t_k)$ for the attractors in Rössler system (2): (a) for the spiral attractor ($a = b = 0.2$, $m = 6.1$) at $D = 0$ (curve *1*), $D = 0.001$ (curve *2*), and $D = 0.1$ (curve *3*); (b) for the funnel attractor ($a = b = 0.2$, $m = 13$) at $D = 0$ (solid curve) and $D = 0.01$ (dashed curve).

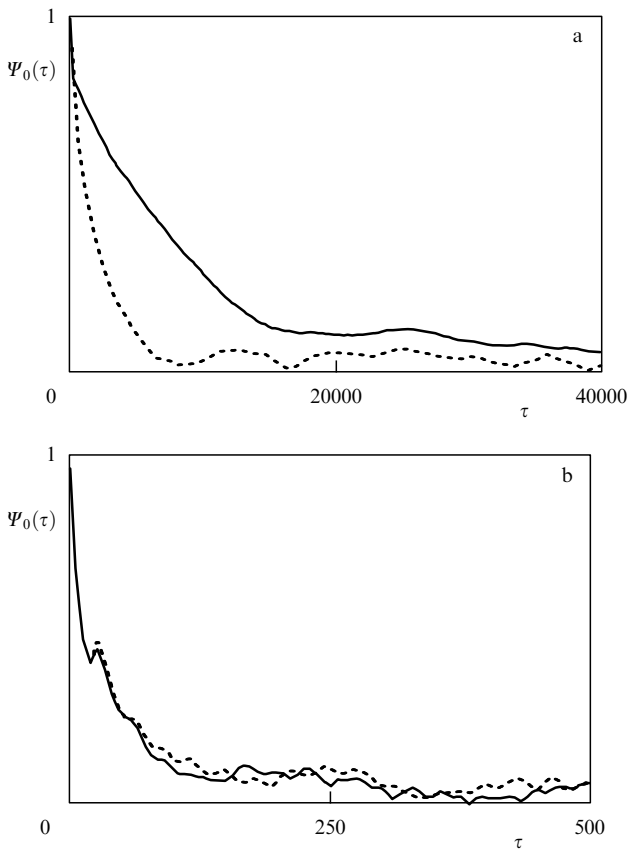

Figure 3. Envelopes of the normalized autocorrelation function $\Psi_0(\tau)$ for the attractors in system (2): (a) at $m = 6.1$, for $D = 0$ (solid curve) and $D = 0.01$ (dashed curve); (b) at $m = 13$, for $D = 0$ (solid curve) and $D = 0.01$ (dashed curve).

not only and not so much by the degree of exponential instability. Other, weightier factors are present. We analyze them below.

For this, we use the notions of instantaneous amplitude and phase of oscillations [77]. Unfortunately, neither is universal. For spiral attractors, these quantities are quite reasonably introduced as

$$x(t) = A(t)\cos\Phi(t)\,, \qquad y(t) = A(t)\sin\Phi(t)\,. \tag{7}$$

As follows from (7), the instantaneous phase is determined by the relation

$$\Phi(t) = \arctan\frac{y(t)}{x(t)} + \pi n(t)\,, \tag{8}$$

where $n(t) = 0, 1, 2, \ldots$ are the numbers of winds of the phase trajectory around the equilibrium state.

We have found that the component of mixing in the direction of the flux of trajectories is associated with the instantaneous-phase variance σ_Φ^2, which controls phase diffusion. Figure 5a illustrates the time dependence of the instantaneous-phase variance σ_Φ^2 on the ensemble of initially close trajectories for the spiral and funnel attractors of system (2). It can be seen that in the time intervals considered, the variance grows in a virtually linear manner both with and without the presence of noise. The assumption that the time dependence of the instantaneous-phase variance for chaotic

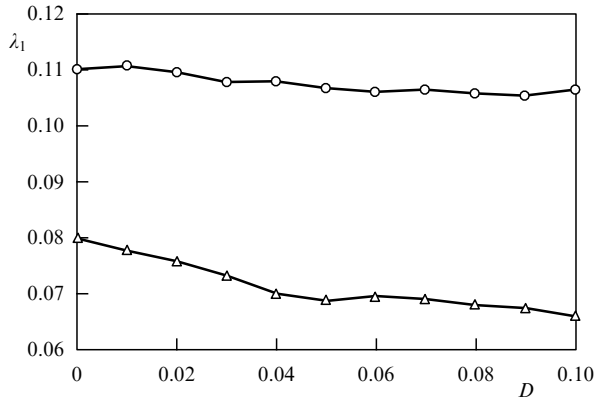

Figure 4. The highest Lyapunov exponent λ_1 in the spiral (triangles) and funnel (circles) attractors as a function of the noise intensity D for the Rössler system.

oscillations in the Rössler system is linear was made in Ref. [75]; however, it was justified neither theoretically nor numerically. For spiral chaos without noise (curve *1*), σ_Φ^2 is small and grows much more slowly than in the other cases under study. The linear growth of the variance allows determining the effective phase-diffusion coefficient (first introduced by Stratonovich [78])

$$B_{\text{eff}} = \frac{1}{2}\left\langle\frac{\mathrm{d}\sigma_\Phi^2(t)}{\mathrm{d}t}\right\rangle, \tag{9}$$

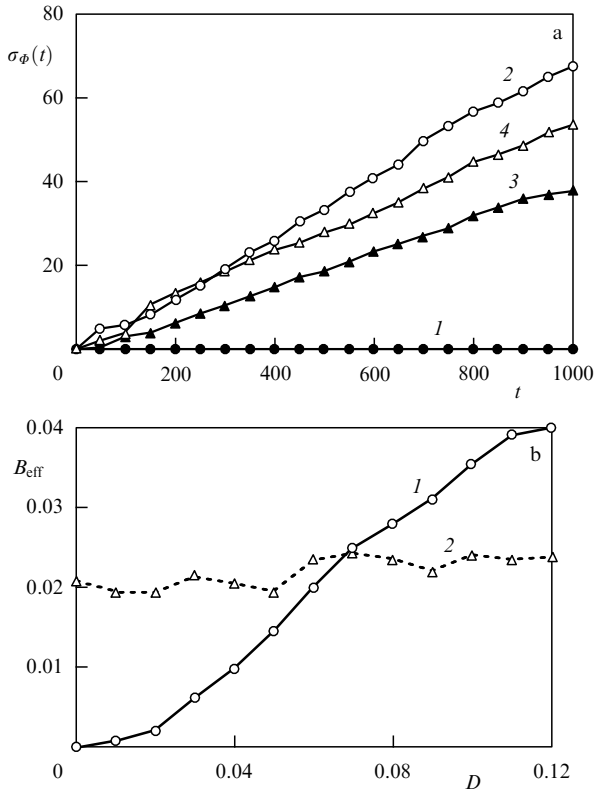

Figure 5. (a) Time dependence of the instantaneous-phase variance σ_Φ^2 for spiral chaos ($m = 6.1$) at $D = 0$ (curve *1*) and $D = 0.1$ (curve *2*) and for incoherent chaos ($m = 13$) at $D = 0$ (curve *3*) and $D = 0.1$ (curve *4*). (b) The effective diffusion coefficient B_{eff} as a function of the noise intensity D for spiral (curve *1*) and incoherent (curve *2*) chaos.

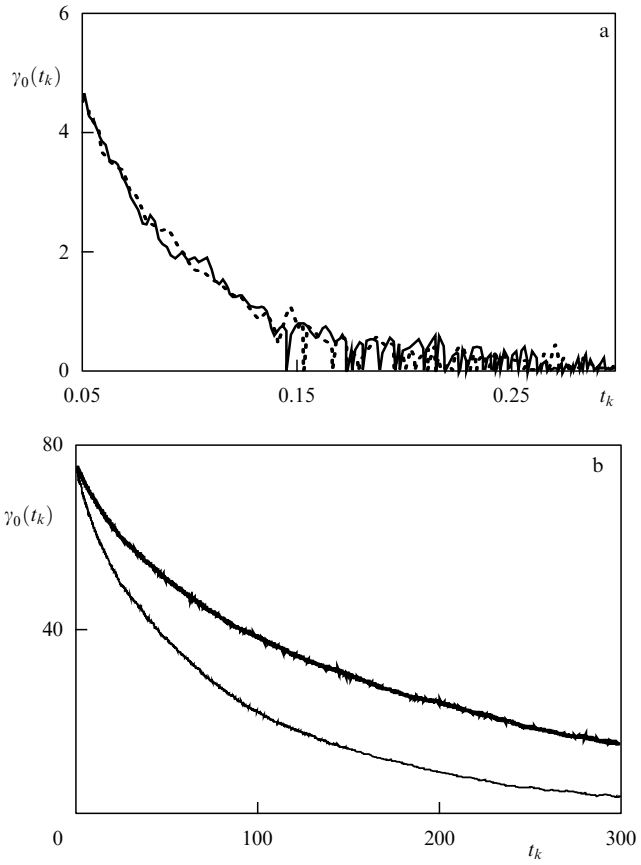

Figure 6. Behavior of the function $\gamma_0(t_k)$ for chaotic attractors in Lorenz system (3): (a) for $r = 28$, $D = 0$ (solid curve) and $D = 0.01$ (dashed curve); (b) for $r = 210$, $D = 0$ (heavy curve) and $D = 0.01$ (light cuvre). The other parameters are $\sigma = 10$ and $\beta = 8/3$.

where the angular brackets denote time averaging of fast oscillations.

The diffusion coefficient B_{eff} as a function of the noise intensity is presented in Fig. 5b for the spiral and funnel attractors in Rössler system (2). It can be seen that B_{eff} grows with D in both cases, but this growth is stronger for spiral chaos.

4.3 Relaxation to the probability measure in the Lorenz system

The well-known quasi-hyperbolic attractors in three-dimensional differential systems, such as the Lorenz attractor and the Shimizu – Morioka attractor [47], are switching-type attracting sets. The phase trajectory switches chaotically from the vicinity of one saddle equilibrium state to the vicinity of another. Such switching involves random phase changes even in the absence of noise. Adding noise does not substantially modify the phase dynamics and does not therefore affect the rate of relaxation to the stationary distribution.

Figure 6 shows the behavior of the function $\gamma_0(t_k)$ for the quasi-hyperbolic and nonhyperbolic chaotic attractors of system (3) with and without the inclusion of noise influences. It has been discovered that noise has virtually no effect on the relaxation rate for the Lorenz attractor (Fig. 6a). The situation is radically different for the nonhyperbolic attractor in the Lorenz system. In this case, noise strongly affects the relaxation rate of the probability measure (Fig. 6b).

We now assess the dependence of the Lyapunov exponent and correlation time on the level of noise influence. For the same chaotic attractors in the Lorenz system, the highest Lyapunov exponent λ_1 and the normalized autocorrelation function $\Psi(\tau)$ ($\tau = t_2 - t_1$) of the dynamical variable $x(t)$ were calculated for various noise intensities D. It was found that within the accuracy of computations, λ_1 is independent of the noise intensity for either type of chaotic attractor. Similarly, noise has virtually no effect on the ACF of the quasi-hyperbolic attractor (Fig. 7a). However, in the regime of the nonhyperbolic attractor, the ACF declines more rapidly with the presence of noise (see the curves in Fig. 7b).

5. Spectral-correlative analysis of dynamical chaos

We now consider the correlative and spectral properties of various types of chaotic oscillations in greater detail. The experience of studying dynamical chaos in three-dimensional differential systems shows that two classical models of random processes can be used to describe the correlative and spectral properties of a certain class of chaotic systems. These are the models of a narrow-band random process (harmonic noise) and of a random telegraphic signal. It was found that the harmonic-noise model describes the correlation parameters of spiral chaos sufficiently well, while the telegraphic-signal model works well for the statistical properties of switching-type attractors, such as the Lorenz attractor [41].

We consider the basic characteristics of the above-mentioned models of random processes.

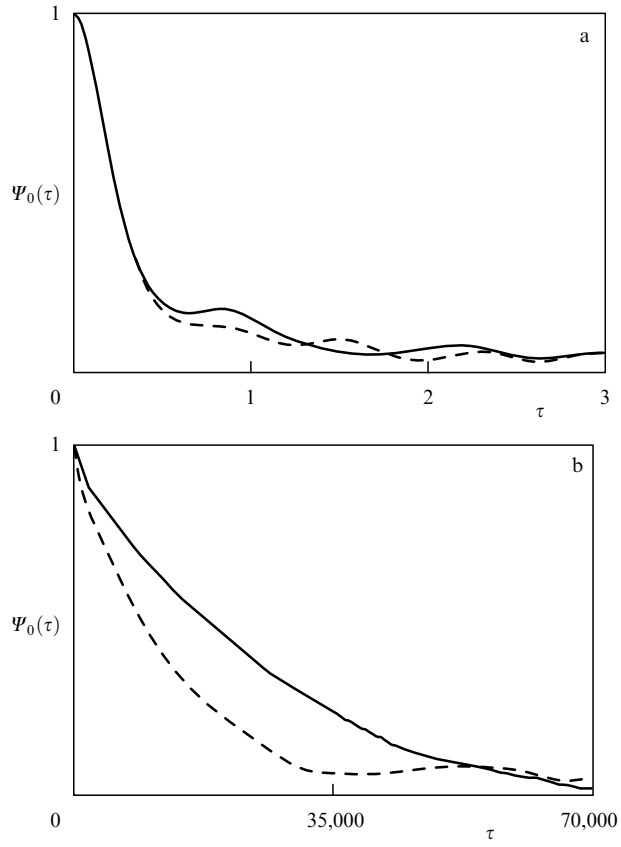

Figure 7. Envelopes of the normalized autocorrelation function $\Psi_0(\tau)$ for the attractors in system (3): (a) $r = 28$, $D = 0$ (solid curve) and $D = 0.01$ (dashed curve); (b) $r = 210$, $D = 0$ (solid curve) and $D = 0.01$ (dashed curve).

Harmonic noise is a narrow-band, zero-mean random process defined by the relation [78–80]

$$x(t) = R_0\big[1 + \alpha(t)\big]\cos\big[\omega_0 t + \phi(t)\big]\,, \tag{10}$$

where R_0 and Ω_0 are constant (mean) values of the amplitude and frequency of oscillations and $\alpha(t)$ and $\phi(t)$ are random functions characterizing the fluctuations of the amplitude and phase of oscillations. The process $\alpha(t)$ is considered to be stationary. The most frequently used simplifying assumptions are as follows: (1) the fluctuations of the amplitude and phase are statistically independent; (2) the phase fluctuations $\phi(t)$ are a Wiener process with a diffusion coefficient B. Under the adopted assumptions, the ACF of process (10) is given by the expression [78–80]

$$\psi(\tau) = \frac{R_0^2}{2}\big[1 + K_\alpha(\tau)\big]\exp\big(-B|\tau|\big)\cos\omega_0\tau\,, \tag{11}$$

where $K_\alpha(\tau)$ is the covariance function of the amplitude fluctuations $\alpha(t)$.[2] The Wiener–Khintchin theorem yields a corresponding expression for the spectral power density.

The *generalized telegraphic signal* is a process that describes random switching between two possible states $x(t) = \pm a$. Two basic types of telegraphic signals — random and quasi-random — can be considered [80, 81]. A random telegraphic signal has a Poisson distribution of switching times t_k, and therefore the probability distribution of pulse lengths is exponential,

$$\rho(\theta) = n_1\exp(-n_1\theta)\,, \qquad \theta \geqslant 0\,, \tag{12}$$

where n_1 is the mean switching frequency. The ACF of such a process decreases exponentially:

$$\psi(\tau) = a^2\exp\big(-2n_1|\tau|\big)\,. \tag{13}$$

The other type of telegraphic signal (quasi-random) corresponds to random switching between two states $x(t) = \pm a$, which is only possible at discrete time instants $t_n = n\xi_0 + \alpha$, $n = 1, 2, 3, \ldots$, where $\xi_0 = \text{const}$ and α is a random quantity. If the probability of switching events is $1/2$, the ACF of this process decays with time according to the linear law

$$\begin{aligned}&\psi(\tau) = a^2\left(1 - \frac{|\tau|}{\xi_0}\right), \qquad |\tau| < \xi_0\,;\\ &\psi(\tau) = 0\,, \qquad |\tau| \geqslant \xi_0\,.\end{aligned} \tag{14}$$

5.1 Spectral-correlative analysis of spiral chaos

From the physical standpoint, spiral-type chaotic attractors largely resemble noisy limit cycles. It should be kept in mind in this context that spiral attractors are present in completely deterministic systems, i.e., without fluctuation sources. We consider the regime of spiral chaos in Rössler system (2) at $a = b = 0.2$ and $m = 6.5$. With this aim in view, we introduced the instantaneous amplitude $A(t)$ and phase $\Phi(t)$ according to (7) and, by means of numerical simulation, we determined the normalized ACF of the chaotic oscillation $x(t)$ (Fig. 8, points in shaded region *1*), the covariance function of amplitude fluctuations $K_A(t)$, and the effective phase-diffusion coefficient B_{eff}. Figure 8 shows the results for $\Psi_x(\tau)$ in system (2) with and without the presence of noise. The decay of the ACF is virtually exponential both in the absence (Fig. 8a) and in the presence of noise (Fig. 8b). Furthermore, as can be seen from Fig. 8c, an interval exists for $\tau < 20$ where the ACF decreases much more rapidly. The envelope of the computed ACF, $\Psi_x(\tau)$, can be approximated using Eqn (11). For this, we substitute the calculated characteristics $K_A(\tau)$ and $B = B_{\text{eff}}$ into the expression for the normalized envelope $\Psi_0(\tau)$:

$$\Psi_0(\tau) = \frac{K_A(\tau)}{K_A(0)}\exp\big(-B_{\text{eff}}|\tau|\big)\,. \tag{15}$$

The calculation results for $\Psi_0(\tau)$ are represented by the points of curves *2* in Figs 8a and 8b. It can be seen that the behavior of the envelope of the ACF, $\Psi_x(\tau)$, is described well by formula (15). We note that taking the factor $K_A(\tau)/K_A(0)$ into account yields a good approximation for all $\tau \geqslant 0$. This means that the amplitude fluctuations are important in short time intervals ($\tau < \tau_{\text{cor}}$), whereas the slow decrease in the correlation is mainly determined by phase diffusion. The surprisingly good agreement between the numerical results for spiral chaos and the data for the classical model of harmonic noise is noteworthy. At the same time, this good agreement is quite difficult to explain. First, relation (11) was obtained under the assumption that the amplitude and phase

[2] The factor $R_0^2\big[1 + K_\alpha(\tau)\big]$ is the covariance function $K_A(\tau)$ of the random amplitude $A(t) = R_0\big[1 + \alpha(t)\big]$. This representation is most convenient to use in our further studies.

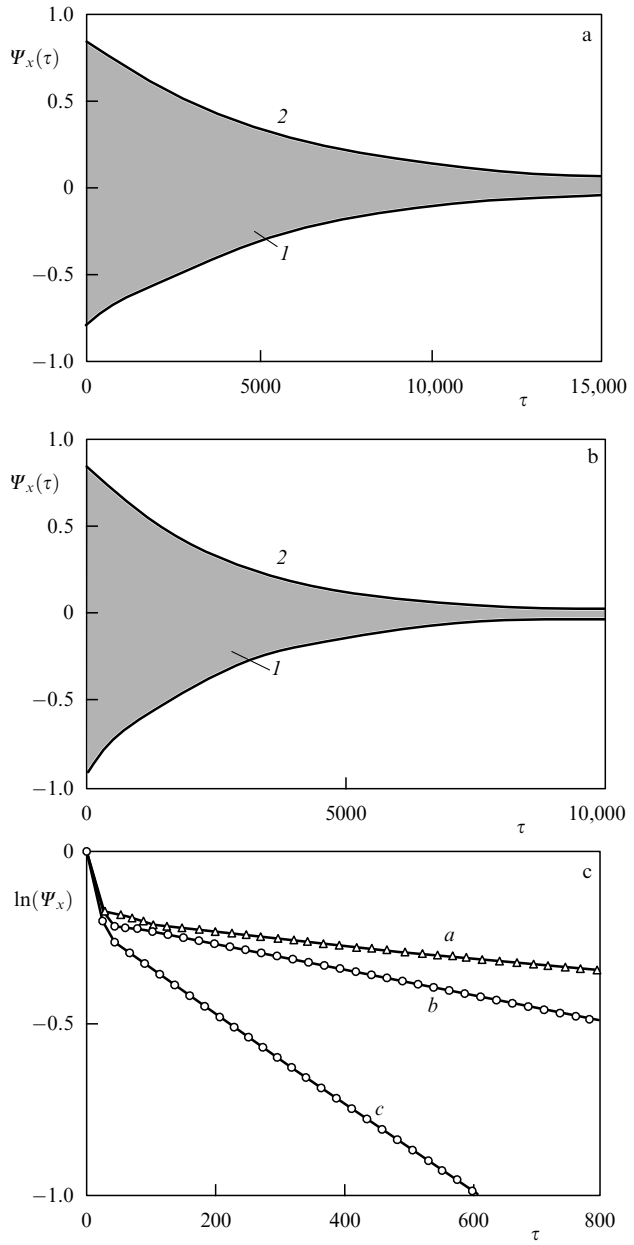

Figure 8. The normalized ACF of the oscillation $x(t)$ in system (2) at $m = 6.5$ (points in the shaded region *1*) and its approximation (15) (points on curve *2*) for $D = 0$ (a) and $D = 10^{-3}$ (b); (c) envelopes of the ACF on a logarithmic scale for $D = 0$ (curve *a*), $D = 0.001$ (curve *b*), and $D = 0.01$ (curve *c*).

fluctuations are statistically independent. It is absolutely clear that this assumption is not applicable to the chaotic regime. Second, formula (11) was derived taking into account that the phase fluctuations can be described in terms of a Wiener process. In the case of chaotic oscillations, $\Phi(t)$ is a more complex process, with unknown statistical properties. It is especially important to emphasize that the results in Fig. 8a were obtained for the regime of purely deterministic chaos (without noise), which additionally confirms the similarity between chaotic self-oscillations and a random process.

It follows from the results presented in Fig. 8 that the envelope of the ACF for chaotic oscillations at $\tau > \tau_{\rm cor}$ can be approximated by the exponential factor $\exp\left(-B_{\rm eff}|\tau|\right)$. According to the Wiener – Khintchin theorem, the spectral peak at the mean frequency ω_0 must have a Lorentzian profile

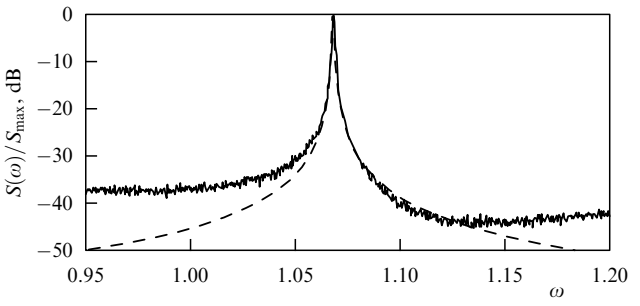

Figure 9. A fragment of the normalized power spectrum of the oscillation $x(t)$ in system (2) at $a = b = 0.2$, $m = 6.5$ (solid curve) and this spectrum approximated by Eqn (16) (dashed curve) for the noise intensity $D = 10^{-3}$.

with the width determined by the effective phase-diffusion coefficient $B_{\rm eff}$:

$$S(\omega) = C\,\frac{B_{\rm eff}}{B_{\rm eff}^2 + (\omega - \omega_0)^2}\,, \qquad C = \text{const}\,. \tag{16}$$

The calculation results shown in Fig. 9 confirm this assertion. The fundamental spectral line can be approximated by expression (16), which is supported by the numerical results for the power spectrum of the oscillation $x(t)$. The results presented in Figs 8 and 9 for the noise intensity $D = 10^{-3}$ were reproduced for various D in the interval $0 < D < 10^{-2}$ and for the range of the parameter m that corresponds to the spiral-chaos regime. We note that the above-presented approximation results for the ACF and the profile of the basic spectral line of the spiral attractor in the Rössler system were completely confirmed by studies of spiral attractors in other dynamical systems [38, 39].

5.2 Correlation parameters of the Lorenz attractor

The narrow-band-noise model cannot be used to analyze the ACFs of switching-type chaotic oscillations, which have a continuous spectrum without pronounced peaks at any distinguished frequencies. Such attractors are quite complex in their structure [82]. The Lorenz attractor is a classical example of a switching-type attractor [41]. We consider the Lorenz system in the quasi-hyperbolic-attractor regime at $r = 28$, $\sigma = 10$, and $\beta = 8/3$.

There are two saddle foci in the phase space of the Lorenz system, which are located symmetrically about the z axis and are separated by the stable manifold of the saddle point at the coordinate origin. The stable manifold has a complex structure, which is responsible for random switching between the saddle foci in peculiar paths [11, 82] (Fig. 10). The phase trajectory, spiraling around a saddle focus, approaches the stable manifold and, with a certain probability, can subsequently enter the vicinity of the other saddle focus. The winding about the saddle foci does not make a significant contribution to the time dependence of the ACF, while the random switching substantially affects the correlation time.

We consider the time dependence of the x coordinate illustrated in Fig. 11. If the winding about the saddle foci is eliminated using the symbolic-dynamics method, we can obtain a signal similar to the telegraphic signal [37, 39].

Figure 12 shows the ACF of the oscillation $x(t)$ for the Lorenz attractor and the ACF of the corresponding telegraphic signal. A comparison between these two graphs indicates that the correlation-decay time and the behavior of

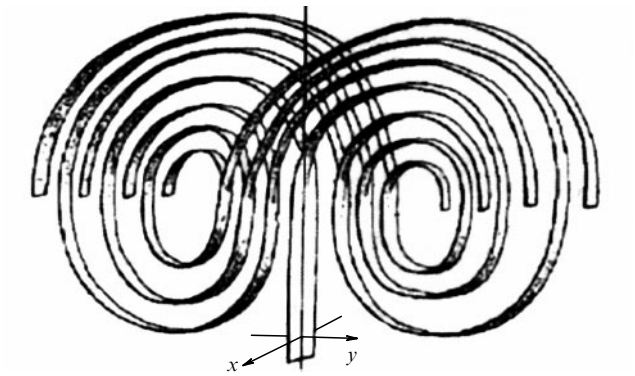

Figure 10. A qualitative illustration of the structure of the manifold in the Lorenz system.

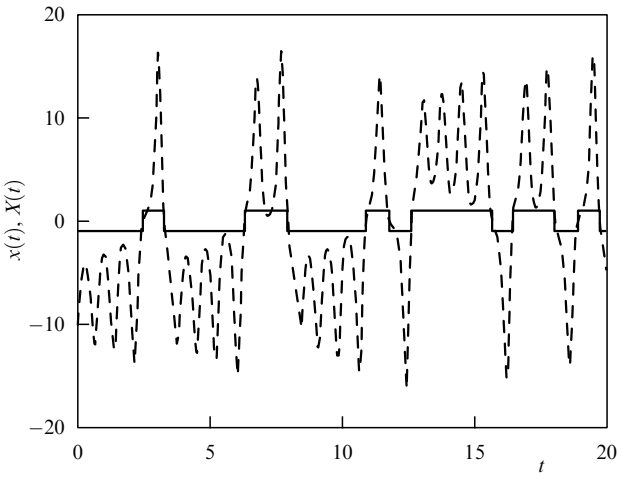

Figure 11. Telegraphic signal (solid curve) obtained for the oscillation $x(t)$ (dashed curve) in the Lorenz system at $\sigma = 10$, $\beta = 8/3$, and $r = 28$.

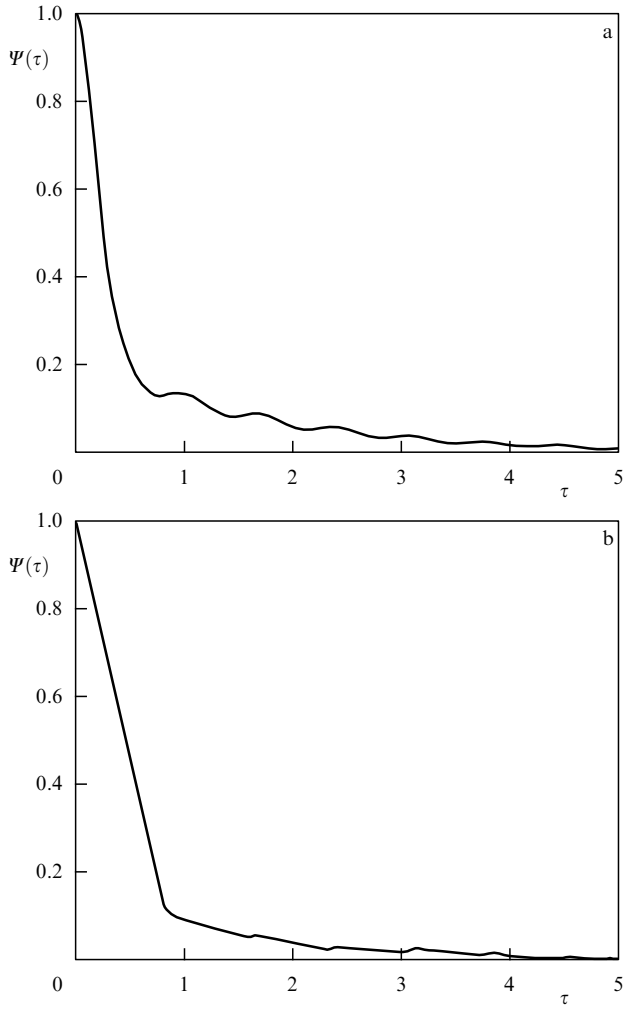

Figure 12. ACF of the oscillation $x(t)$ (a) and the telegraphic signal (b).

the ACF on this time scale are mainly determined by the switching, while the winding about the saddle foci does not contribute considerably to the ACF decay. It is important to note that the ACF decay law is virtually linear at short times. This fact is remarkable, because a linear decay of the ACF corresponds to a discrete equidistant probability distribution of residence times in the form of a set of delta peaks, and the probability of switching between two states should be $1/2$ [80, 81].

Figure 13 shows the distribution of residence times computed for the telegraphic signal presented in Fig. 11. As can be seen from Fig. 13a, the distribution of residence times indeed has a structure close to an equidistant discrete distribution. At the same time, the peaks are not δ-like spikes but have finite widths. Figure 13b shows the probability distribution of switching that occurs at values that are multiples of ξ_0, the minimum residence time for one state.[3] This dependence demonstrates that the probability of a transition within the time ξ_0 (within one trajectory winding) is close to $1/2$. The discrete character of switching can be accounted for by the properties of the manifold structure in the Lorenz system (see Fig. 10). The manifolds split into two sheets near the origin $x = 0$, $y = 0$. As a result, the probability of switching between two states within one winding about a fixed point is approximately $1/2$. Because of this particular aspect of the dynamics, the ACF of the oscillations $x(t)$ and $y(t)$ on the Lorenz attractor has the form specified by expression (14). However, the finite width of the distribution peaks and deviations of the probability $P(\xi_0)$ from $1/2$ can result in the ACF not linearly decreasing to zero (see Fig. 13).

[3] The time ξ_0 corresponds to the duration of one trajectory winding about the saddle focus in the Lorenz attractor.

6. Phase diffusion in an active inhomogeneous medium described by the Ginzburg–Landau equation

Distributed systems are among the most interesting subjects of investigation in theoretical physics. First and foremost, this is due to wave processes that occur only in distributed systems. Numerous studies have been dedicated to the dynamics of continuous media, including the onset of turbulence. An irregular behavior of the medium in space and time can develop because of its spatial nonuniformity [83–85]. Effects of spatial nonuniformity have been studied, for example, in ensembles of coupled self-oscillatory systems [86, 87] that can be regarded as models approximating a distributed active medium. In ensembles with a spatial frequency gradient, the emergence of frequency clusters — groups of oscillators with equal or close mean frequencies —

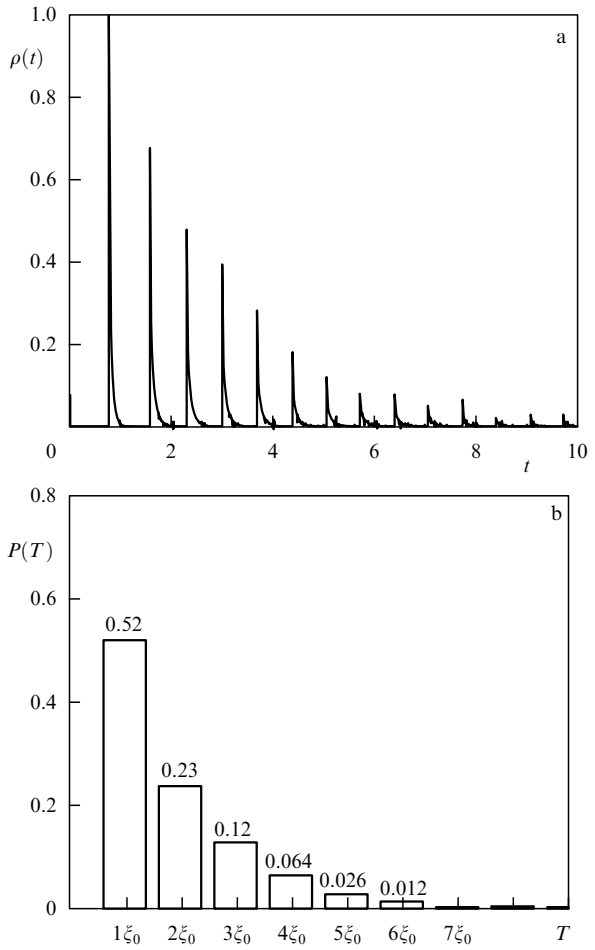

Figure 13. The distribution of pulse durations for the telegraphic signal (a) and the probability distribution of switching within times that are multiples of ξ_0 (b).

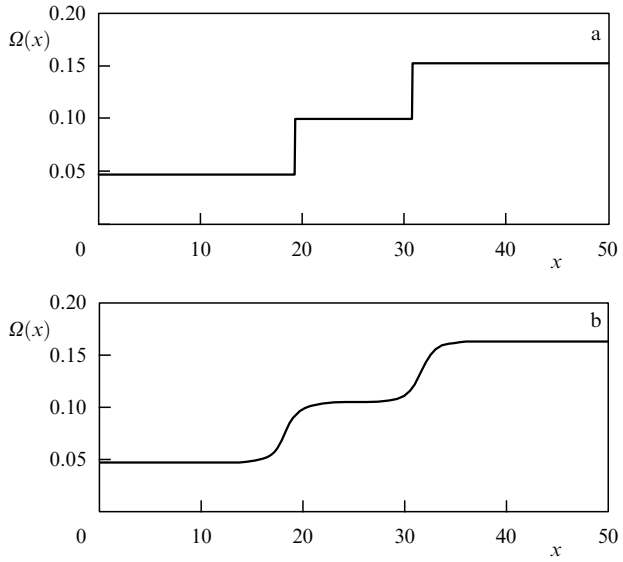

Figure 14. Variation in the mean oscillation frequency Ω along the medium for a perfect cluster structure at $g = 1.0$ (a) and for an imperfect structure at $g = 0.85$ (b).

is typical. Accordingly, perfect (with equal frequencies) or imperfect (with differing frequencies) clusters are considered.

Frequency clusters can also form in a continuous inhomogeneous active medium [88, 89]. In contrast to ensembles, which consist of discrete sets of oscillators, a regime with a continuous coordinate dependence of the frequency is possible in a medium with imperfect clusters. This corresponds to the effect of emergence of imperfect clusters with a continuous power spectrum of oscillations. Because this phenomenon can be observed in a purely deterministic medium in the absence of fluctuations, it implies the onset of deterministic chaos in a distributed medium. We here consider the onset of chaotic temporal behavior of a continuous inhomogeneous medium and compare the details of the dynamics of the inhomogeneous medium with the above-described emergence of phase diffusion in finite-dimensional systems.

As an example, we studied a one-dimensional self-oscillatory medium that obeys the Ginzburg – Landau equation with a coordinate-dependent frequency,

$$a_t = \mathrm{i}\omega(x)a + \frac{1}{2}\left(1 - |a|^2\right)a + g a_{xx}\,, \qquad (17)$$

where i is the imaginary unit, $a(x, t)$ is the complex amplitude of oscillations, t is the time, $x \in [0, l]$ $(l = 50)$ is the spatial coordinate, and g is the diffusion coefficient.

As $g \to 0$, oscillations at different points of the medium have different frequencies specified by the function $\omega(x)$. We considered the case where the frequency depends on the spatial coordinate linearly, $\omega(x) = x\Delta_{\max}$; in experiments, $\Delta_{\max}$ was set to the fixed value 0.2. The boundary conditions had the form

$$a_x(x, t)\Big|_{x=0;\,l} \equiv 0\,.$$

The initial state of the medium was chosen at random near some uniform distribution $a_0 = \mathrm{const}$. Equation (17) was integrated numerically using an implicit finite-difference technique with a forward – backward marching procedure [90]. We calculated the real oscillation amplitude

$$A(x, t) = \left|a(x, t)\right|$$

and the phase

$$\phi(x, t) = \arg a(x, t)\,.$$

The mean oscillation frequency was computed as the mean time derivative of the phase,

$$\Omega(x) = \left\langle \phi_t(x, t) \right\rangle .$$

If no mismatch is present ($\Delta_{\max} = 0$), only uniform self-oscillation regimes are possible in medium (17): $a(x, t) \equiv a(t)$. At a given mismatch $\Delta_{\max}$, the formation of perfect and imperfect frequency clusters can be observed in a certain range of diffusion-coefficient values (Fig. 14). Time-periodic oscillations correspond to perfect clusters. In the regime of imperfect clusters, the time variation in the oscillation amplitude A at any fixed point in the medium x is quite complicated and resembles a chaotic process.

This effect can be illustrated by the calculations of the power spectra for the regimes of perfect and imperfect clusters shown in Fig. 15. As the regime evolves from perfect to imperfect clusters, a transition from multifrequency regular oscillations to complicated oscillations with a continuous spectrum are observed in the medium at any spatial point.

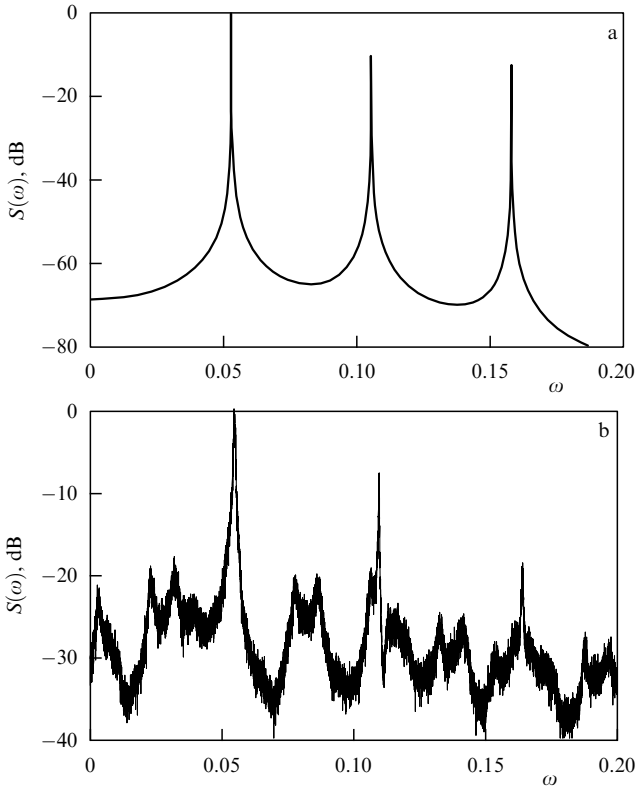

Figure 15. Normalized spectral power densities of the process $A(x_{1,2}, t)$: (a) in the regime of perfect clusters ($g = 1.0$) at the point $x_1 = 25$ (cluster center); (b) in the regime of imperfect clusters ($g = 0.85$ at the point $x_1 = 25$) (cluster center).

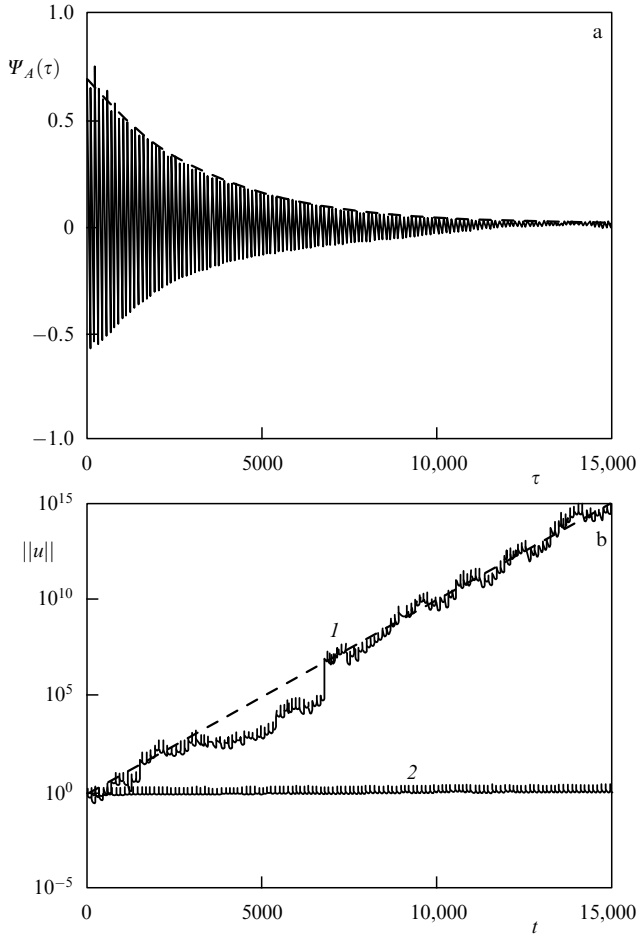

Figure 16. (a) The normalized autocorrelation function of the process $A(x, t)$ in the regime of imperfect clusters ($g = 0.85$) at the point $x = 25$ (cluster center). The dashed curve represents the exponential approximation of the envelope of the ACF: $C\exp(-\alpha\tau)$, $\alpha = 0.0003$, $C = \text{const}$. (b) Time dependence of the perturbation norm $\|u(x, t)\|$ for the oscillation of medium (17) in the regime of imperfect frequency clusters at $g = 0.85$ (curve *1*) and in the regime of perfect frequency clusters at $g = 1.00$ (curve *2*). The dashed straight line corresponds to the exponential function $\exp(0.0023t)$.

We also calculated the temporal ACFs of the process $A(x, t)$ for various points in the medium,

$$\psi_A(x, \tau) = \big\langle A(x, t)A(x, t + \tau)\big\rangle - \big\langle A(x, t)\big\rangle^2 , \qquad (18)$$

where the angular brackets $\langle\ \rangle$ denote time averaging and $\big\langle A(x, t)\big\rangle$ is t-independent. We considered the normalized ACF (correlation coefficient)

$$\Psi_A(x, \tau) = \frac{\psi_A(x, \tau)}{\psi_A(x, 0)} .$$

An ACF is exemplified in Fig. 16a. Our calculations demonstrate that in the imperfect-cluster regime, $\Psi_A(x, \tau)$ decreases with time at any point in the medium x, ultimately approaching zero (Fig. 16a). This testifies to the presence of mixing. Two time scales can be distinguished in the ACF-envelope decay law. At small τ (of several oscillation periods), the correlation declines rapidly. At longer times, an exponential decrease with a certain damping rate α is a fairly good approximation. The damping rate varies within the range $\alpha = (0.15-0.4) \times 10^{-3}$, depending on the point in the medium. If the cluster structure is perfect, periodic or quasi-periodic processes occur in the medium, with corresponding correlation functions.

Because no noise sources are present in the model under study, only the onset of dynamical chaos — an absolute exponential instability of oscillations in the medium — can be responsible for mixing. To analyze the stability of the oscillations, we jointly integrated Eqn (17) and the linearized equation for a small perturbation $u(x, t)$ of the complex amplitude $a(x, t)$:

$$u_t = \mathrm{i}\omega(x)u + \frac{1}{2}\big(1 - |a|^2\big)u - \frac{1}{2}\,a^2u^* + gu_{xx} , \qquad (19)$$

where u^* is complex conjugate to u. The boundary conditions for the perturbation are given by

$$u_x(x, t)\Big|_{x=0;\,l} \equiv 0 .$$

For any time t, the Euclidean perturbation norm $\|u(x, t)\|$ was considered, which reduced to the sum of a finite number of terms because of the discretization of the spatial coordinate. Our calculations have shown that the decay of the ACF in the regime of imperfect clusters is accompanied by an exponential temporal growth (on average) in the perturbation norm (Fig. 16b). The rate of the exponential growth $\lambda_{\max}$ obtained for $g = 0.85$ had the value $\lambda_{\max} \approx 0.0023$. We note that this $\lambda_{\max}$ exceeds the damping rate of the ACF by an order of magnitude.

To check the presence of exponential instability in the medium, we calculated the highest Lyapunov exponent $\lambda_{\max}$, based on the time series of data, using the algorithm suggested

in [91]. The calculations yielded a positive value of the highest Lyapunov exponent, which weakly depends on the parameters of the numerical scheme. The results corresponding to different points in the medium differed to a certain extent but were all of the order 10^{-3}. For instance, at the optimum parameters of the numerical scheme, the reconstruction technique yielded

$$\lambda_{\max} = 0.002 \pm 0.0002$$

for the point $x_1 = 25$, which agrees very well with the results of the linear stability analysis. Thus, it can be safely said that the regime of imperfect frequency clusters corresponds to chaotic oscillations in time.

The estimates of the highest Lyapunov exponent obtained using two different methods agree well with each other, but differ substantially (by an order of magnitude) from the estimate for the exponential-damping rate of the correlations in the corresponding regime. According to the above discussion, for a broad class of chaotic systems with lumped parameters, the rate of correlation splitting at long time intervals and the width of the main spectral line are determined by the effective diffusion coefficient for the instantaneous phase of the fluctuations,

$$y(t) = A(t) - \langle A(t) \rangle .$$

To verify this assertion, we studied the dynamics of the instantaneous phase defined as

$$\Phi(t) = \arctan\left(\frac{y_{\rm h}(t)}{y(t)}\right) \pm \pi k , \qquad k = 0, 1, 2, \ldots , \tag{20}$$

where $y_{\rm h}(t)$ is the Hilbert-conjugate process. The choice of an integer k in Eqn (20) is dictated by the continuity condition for the function $\Phi(t)$.

For an ensemble of segments of a sufficiently long realization $\Phi(t)$, we calculated the variance

$$\sigma_\Phi^2(t) = \langle \Phi^2(t) \rangle - \langle \Phi(t) \rangle^2$$

where the angular brackets $\langle\ \rangle$ denote ensemble averaging. The variance of the instantaneous phase is plotted as a function of time in Fig. 17. The variance grows with time almost linearly in the interval $t \in [0, 10000]$. A least-square estimate of the angular growth factor makes it possible to determine the effective diffusion coefficient for the phase $\Phi(t)$:

$$B_{\rm eff} = \frac{1}{2}\left\langle \frac{{\rm d}\sigma_\Phi^2(t)}{{\rm d}t} \right\rangle . \tag{21}$$

Here, the angular brackets $\langle\ \rangle$ denote averaging 'fast' variance oscillations over time.

In the regime of imperfect clusters, the obtained $B_{\rm eff}$ values range within the interval $[0.00016, 0.00038]$, depending on the spatial coordinate x. A more accurate, direct calculation of $B_{\rm eff}$ based on formula (21) proved to be quite complicated because of the need of averaging over a vast dataset.

Our numerical investigation revealed a number of important new facts.

(1) The development of chaos and turbulence in a continuous self-oscillatory medium can result from the inhomogeneity of the medium, which specifies a continuous coordinate dependence of the self-oscillation frequency.

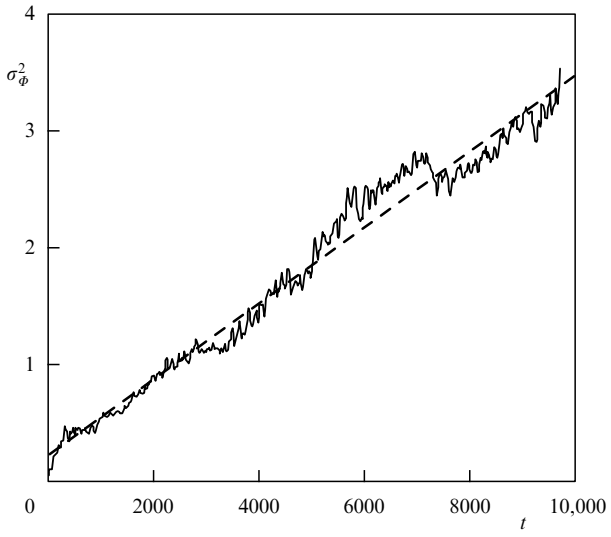

Figure 17. Dispersion of the instantaneous phase computed for the regime of imperfect clusters ($g = 0.85$) at the point $x = 25$ (cluster center), $B_{\rm eff} \approx 0.00016$. The approximating straight line is shown dashed.

(2) The self-oscillations of the medium in the regime of imperfect, partial (cluster) synchronization are mixable, i.e., they are exponentially unstable, with split temporal correlations.

(3) The damping rate of the correlation functions at long times is not directly determined by the Lyapunov exponent but is related to the diffusion of the instantaneous oscillation phase. This testifies to the generality of the correlation splitting laws in finite-dimensional and distributed chaotic systems.

7. The autocorrelation function and power spectrum of spiral chaos in physical experiments

Our experiments were carried out using a setup that included a radiotechnical generator with inertial nonlinearity (Anishchenko – Astakhov generator [43]) and the fundamental frequency 18.5 kHz, a fast-ADC computer with the discretization frequency 694.5 kHz, and a generator of broadband Gaussian noise in the frequency band from 0 to 100 kHz [92]. The behavior of the ACF was also analyzed in the presence of external noise. With this aim in view, a signal from an external noise generator with controlled noise intensity was fed to the system. The generator with inertial nonlinearity can be described by the three-dimensional dissipative dynamical system

$$\dot{x} = mx + y - xz - \delta x^3 , \qquad \dot{y} = -x , \qquad \dot{z} = -gz + gI(x)x^2 ,$$
$$I(x) = \begin{cases} 1 , & x > 0 , \\ 0 , & x \leqslant 0 . \end{cases} \tag{22}$$

At certain m and g, the system realizes spiral-chaos regimes [43].

The first important question to be unambiguously resolved in the experiment is whether the Wiener-process approximation can be used to describe the statistical parameters of the instantaneous phase, as assumed in Refs [21, 37,

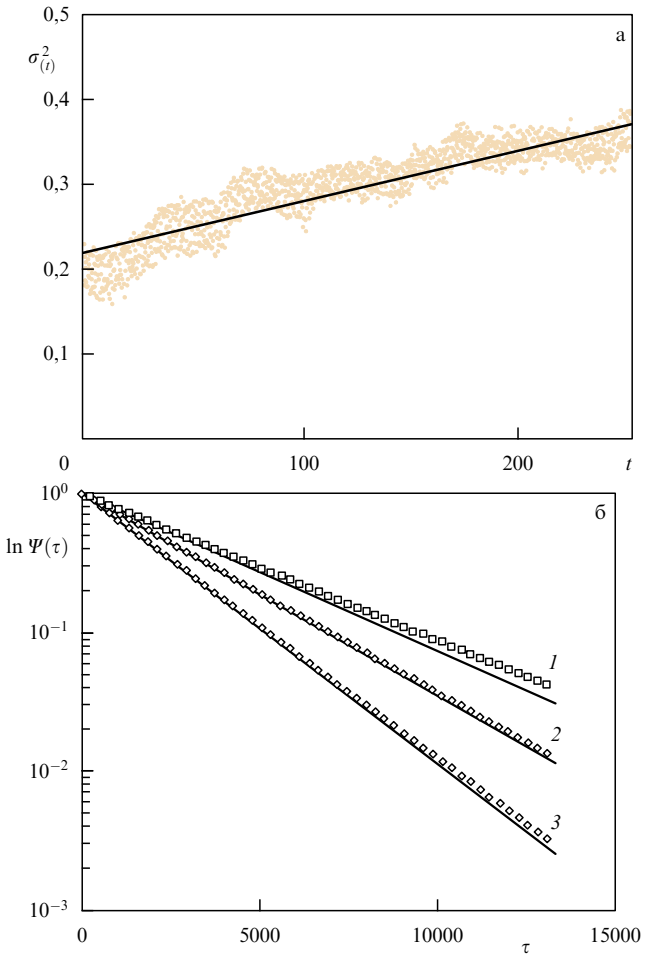

Figure 18. (a) Time dependence of the phase variance in the presence of noise with the intensity $D = 0.001$ mV and the linear least-square approximation of this dependence (the dimensionless time t is equal to the number of oscillation periods). (b) The ACF envelopes (solid lines) obtained experimentally for various intensities of the external noise: *1*, $D = 0$; *2*, $D = 0.0005$ mV; and *3*, $D = 0.001$ mV; with their experimental approximations (straight lines) for the respective damping rates $B_{\text{eff}} = 0.00024$, $B_{\text{eff}} = 0.00033$, and $B_{\text{eff}} = 0.000439$. The other parameters of the numerical calculations are $N = 100$, $n = 262144$, and $p = 1/(2n)$.

39, 75]. The instantaneous phase used to determine the diffusion coefficient B_{eff} is based on the concept of an analytical signal with the application of the Hilbert transform of experimental realizations of $x(t)$ [77]. The phase variance $\sigma^2_{\Phi}(t)$ is then computed by averaging over an ensemble of N realizations. The effective phase-diffusion coefficient is determined by the temporal-growth rate of the variance.

The time dependence of the phase diffusion shown in Fig. 18a is not strictly linear, as should be expected for a Wiener process. However, the linear growth dominates over small fluctuations in the phase variance. Therefore, the process under consideration can be associated with a Wiener process whose diffusion coefficient is B_{eff}.

The next stage of the experiment is the measurement of the ACF for the chaotic oscillations of the generator with inertial nonlinearity. Several dozen realizations of the signal $x(t)$, each with a duration of 10 s, were recorded by the fast ADC. The total length of the realization was $(3-5) \times 10^5$ oscillation periods with a discretization step Δt corresponding to 37 points per period. The ACF was calculated as follows. First, we computed the time-averaged value of the x variable for each of N realizations of the process $x(t)$:

$$\bar{x} = \frac{1}{n}\sum_{i=1}^{n} x(t_i)\,. \tag{23}$$

Next, time averaging was used to obtain the mean product $\langle x(t)x(t+\tau)\rangle$,

$$K_l(\tau) = \frac{1}{p}\sum_{i=1}^{p} x(t_i)x(t_i + k\Delta t)\,, \qquad \tau = k\Delta t_i\,, \quad k = 0, 1, \ldots, n-p\,, \tag{24}$$

where $l = 1, \ldots, N$ is the realization number. Because the correlation-decay rate is not high in the regime under consideration, the ACF should be calculated for a very long time interval. To achieve high accuracy in the calculation of the ACF, the obtained data were averaged over N realizations:

$$\psi(\tau) = \frac{1}{N}\sum_{l=1}^{N} K_l(\tau) - \bar{x}^2\,. \tag{25}$$

The ACF was normalized to the maximum value at $\tau = 0$, i.e.,

$$\Psi(\tau) = \frac{\psi(\tau)}{\psi(0)}\,.$$

Experimental graphs of the envelopes of the normalized ACF for various external-noise intensities are shown in Fig. 18b. The obtained dependences were approximated by the exponential law

$$\Psi_{\text{app}}(\tau) = \exp\left(-B_{\text{eff}}\tau\right),$$

where B_{eff} is the experimentally determined effective instantaneous-phase diffusion coefficient. The approximations are shown by symbols in Fig. 18b.

We now analyze the results of the power-spectrum measurements. The power spectrum of a diffusive process has a Lorentzian profile whose width is determined by the effective phase-diffusion coefficient. For a normalized spectrum, the Lorentzian is given by formula (16). Experimentally, the diffusion coefficient can be independently determined by measuring the width of the spectral peak. To obtain a more accurate value of the diffusion coefficient, we approximated the spectral peak using formula (16) and varying B_{eff}. We chose the B_{eff} value at which the approximation error was minimum (Fig. 19a). Figure 19 presents experimental power spectra of the generator with inertial nonlinearity. The spectrum was computed using the standard technique of the fast Fourier transform (FFT) with averaging. The principal result is that the values of the effective phase-diffusion coefficient based on the power-spectrum measurements agree well with the B_{eff} values obtained from the linear approximation of the growth of the instantaneous-phase variance. The corresponding values of the effective phase-diffusion coefficient are given in the table for three values of the external-noise intensity.

Thus, we have found experimentally that in the spiral-chaos regime, the instantaneous-phase variance of chaotic oscillations grows on average linearly with the diffusion coefficient B_{eff}. In the absence of noise, this coefficient is

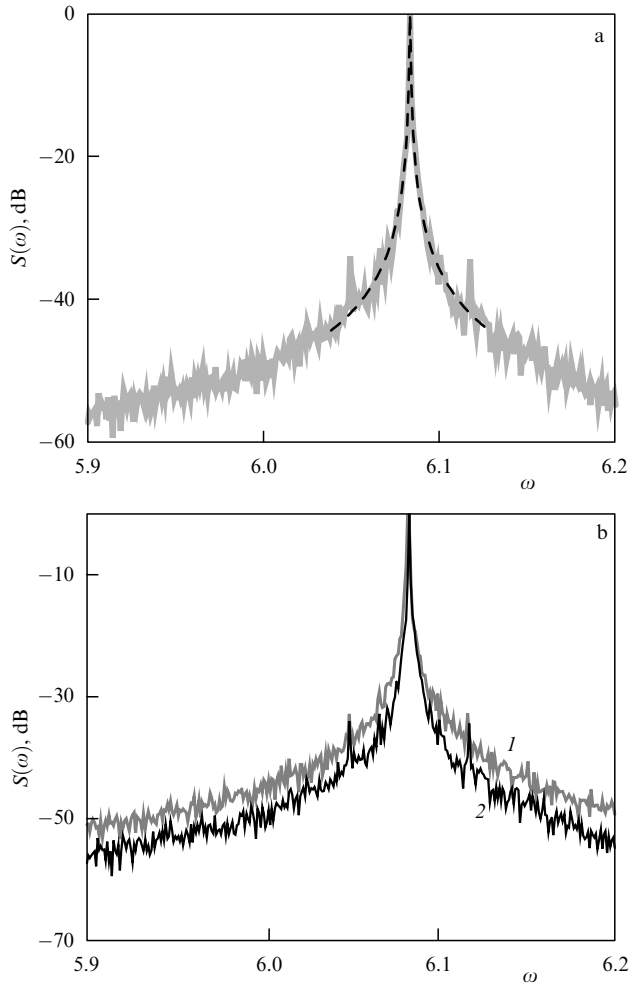

Figure 19. (a) Experimentally obtained power spectrum of the oscillation $x(t)$ in system (22) and its theoretical approximation (16) at $B_{\text{eff}} = 0.00033$ in the presence of noise with $D = 0.0005$; (b) power spectra for $D = 0.001$ (curve *1*) and $D = 0$ (curve *2*).

Table. Comparison of the phase-diffusion coefficients obtained using various techniques with the inclusion of noise of varying intensity.

D, mV	B_{eff} (Hilbert)	B_{eff} (spectrum)
0	0.000244	0.000266
0.0005	0.00033	0.000342
0.001	0.000439	0.000443

controlled by the chaotic dynamics of the system. If noise is present, the growth of the phase variance is also linear, but B_{eff} increases. The ACF of spiral chaos decreases exponentially with time, as $\exp(-B_{\text{eff}}\tau)$. The spectral-line width of oscillations at the fundamental frequency ω_0 is determined by the phase-diffusion coefficient according to Eqn (16).

8. Conclusion

Our results demonstrate the existence of a class of spiral-type nonhyperbolic attractors for which noise has a pronounced effect on the rate of relaxation to the stationary distribution and on the correlation time but, virtually, does not influence the value of the positive Lyapunov exponent. The rate of mixing on nonhyperbolic attractors is determined not only and not very much by the exponential instability but depends on the complex dynamics of the instantaneous phase of chaotic oscillations. In the spiral-chaos regime, noise substantially increases the rate of relaxation to the stationary distribution. For chaotic attractors with an irregular behavior of the instantaneous phase, noise has virtually no effect on the mixing rate. This is the case for nonhyperbolic funnel and switching-type attractors such as the quasi-hyperbolic Lorenz attractor.

Spiral nonhyperbolic attractors can appear not only in finite-dimensional but also in distributed systems. An inhomogeneous medium modeled by the Ginzburg – Landau equation can serve as an example. A characteristic feature of spiral attractors is that they correspond to a complex process of irregular self-oscillations whose statistical properties can be described in terms of the classical model of narrow-band noise. In essence, spiral chaos is similar in its properties to a noisy limit cycle (e.g., a noise-affected Van der Pol generator). The autocorrelation function and power spectrum of a spiral attractor are completely determined by the fluctuations in the instantaneous amplitude and phase of oscillations. The amplitude fluctuations control the decay rate of the correlations at short time intervals and, accordingly, the noise pedestal in the power spectrum. The phase fluctuations broaden the spectral line at the fundamental frequency in the spectrum and result in an exponential decay in the autocorrelation function, which is determined by the effective diffusion coefficient B_{eff}. The phase-diffusion coefficient in a noise-free system is determined by its chaotic dynamics and does not directly depend on the positive Lyapunov exponent. The following important conclusion can be deduced: in dynamical systems with spiral chaos, the Kolmogorov entropy as a quantitative characteristic of the mixing rate is mainly controlled by the growth rate B_{eff} of the instantaneous-phase variance rather than by the positive Lyapunov exponent, as is generally assumed. Analyses of the statistical properties of the Lorenz attractor have shown that the properties of the ACF are mainly determined by the random-switching process, weakly depending on winding about the saddle foci. The classical model of the telegraphic signal can be used to describe the statistics of the Lorenz attractor. In particular, this model provides a good approximation of the interval of linear decrease in the ACF, which enables us to theoretically calculate the correlation time. The fact that the ACF decay rate for the Lorenz attractor is virtually constant both in and without the presence of noise results from the statistics of the switching process. The probability of switching in the Lorenz attractor is nearly 1/2 and virtually independent of the level of noise influence.

Acknowledgments

This work was supported by the BRHE Program 'Basic Research and Higher Education' (project code SR-006-Xl), the Russian Foundation for Basic Research (project code 04-02-16283), and the Ministry of Education and Science of the Russian Federation (project code E02-3.2-345).

References

1. Anosov D V *Trudy Mat. Inst. im. V.A. Steklova Akad. Nauk SSSR* **90** 3 (1967) [*Proc. Steklov Inst. Math.* **90** 1 (1967)]
2. Smale S *Bull. Am. Math. Soc.* **73** 747 (1967)
3. Ruelle D, Takens F *Commun. Math. Phys.* **20** 167 (1971)
4. Guckenheimer J, Holms P *Nonlinear Oscillations, Dynamical Systems, and Bifurcations of Vector Fields* (New York: Springer-Verlag, 1983)

5. Sinaĭ Ya G *Usp. Mat. Nauk* **25** 141 (1970) [*Russ. Math. Surv.* **25** 137 (1970)]
6. Sinaĭ Ya G, in *Nelineĭnye Volny* (Nonlinear Waves) (Ed. A V Gaponov-Grekhov) (Moscow: Nauka, 1979) p. 192
7. Bunimovich L A, Sinaĭ Ya G, in *Nelineĭnye Volny* (Nonlinear Waves) (Ed. A V Gaponov-Grekhov) (Moscow: Nauka, 1979) p. 212
8. Eckmann J-P, Ruelle D *Rev. Mod. Phys.* **57** 617 (1985)
9. Ruelle D *Am. J. Math.* **98** 619 (1976)
10. Ruelle D *Bol. Soc. Bras. Math.* **9** 83 (1978)
11. Shilnikov L *Int. J. Bifurcat. Chaos* **7** 1953 (1997); *J. Circuits Syst. Comput.* **3** 1 (1993)
12. Afrajmovich V S, Shil'nikov L P, in *Nonlinear Dynamics and Turbulence* (Eds G I Barenblatt, G Iooss, D D Joseph) (Boston: Pitman, 1983) p. 1
13. Anishchenko V S, Strelkova G I *Discrete Dyn. Nat. Soc.* **2** 53 (1998)
14. Graham R, Ebeling W, private communications; Graham R, Hamm A, Tél T *Phys. Rev. Lett.* **66** 3089 (1991)
15. Ott E, Yorke E D, Yorke J A *Physica D* **16** 62 (1985)
16. Schroer C G, Ott E, Yorke J A *Phys. Rev. Lett.* **81** 1397 (1998)
17. Sauer T, Grebogi C, Yorke J A *Phys. Rev. Lett.* **79** 59 (1997)
18. Jaeger L, Kantz H *Physica D* **105** 79 (1997)
19. Kifer Yu *Commun. Math. Phys.* **121** 445 (1989); *Izv. Akad. Nauk SSSR Ser. Mat.* **38** 1091 (1974)
20. Hammel S M, Yorke J A, Grebogi C *J. Complexity* **3** 136 (1987); *Bull. Am. Math. Soc., New Ser.* **19** 465 (1988)
21. Anishchenko V S et al. *Phys. Rev. Lett.* **87** 054101 (2001)
22. Anishchenko V S et al. *Phys. Rev. E* **65** 036206 (2002)
23. Zaslavsky G M *Chaos in Dynamical Systems* (New York: Harwood Acad. Publ., 1985)
24. Billingsley P *Ergodic Theory and Information* (New York: Wiley, 1965)
25. Cornfeld I P, Fomin S V, Sinai Ya G *Ergodic Theory* (New York: Springer-Verlag, 1982)
26. Kolmogorov A N *Dokl. Akad. Nauk SSSR* **124** 754 (1959)
27. Sinaĭ Ya G *Dokl. Akad. Nauk SSSR* **124** 768 (1959)
28. Pesin Ya B *Usp. Mat. Nauk* **32** (4) 55 (1977) [*Russ. Math. Surv.* **32** (4) 55 (1977)]
29. Bowen R *Equilibrium States and the Ergodic Theory of Anosov Diffeomorphisms* (Lecture Notes in Math., Vol. 470) (Berlin: Springer-Verlag, 1975)
30. Blank M L *Ustoĭchivost' i Lokalizatsiya v Khaoticheskoĭ Dinamike* (Stability and Localization in Chaotic Dynamics) (Moscow: Izd. MTsNMO, 2001)
31. Ruelle D *Commun. Math. Phys.* **125** 239 (1989)
32. Christiansen F, Paladin G, Rugh H H *Phys. Rev. Lett.* **65** 2087 (1990)
33. Liverani C *Ann. Math.* **142** 239 (1995)
34. Froyland G *Commun. Math. Phys.* **189** 237 (1997)
35. Bowen R, Ruelle D *Invent. Math.* **29** 181 (1975)
36. Badii R et al. *Physica D* **58** 304 (1992)
37. Anishchenko V S et al. *Physica A* **325** 199 (2003)
38. Anishchenko V S et al. *Fluct. Noise Lett.* **3** L213 (2003)
39. Anishchenko V S et al. *Radiotekh. Elektron.* **48** 824 (2003) [*J. Commun. Technol. Electron.* **48** 750 (2003)]
40. Rössler O E *Phys. Lett. A* **57** 397 (1976)
41. Lorenz E N *J. Atmos. Sci.* **20** 130 (1963)
42. Anishchenko V S *Slozhnye Kolebaniya v Prostykh Sistemakh* (Complex Oscillations in Simple Systems) (Moscow: Nauka, 1990)
43. Anishchenko V S *Dynamical Chaos — Models and Experiments* (Singapore: World Scientific, 1995)
44. Williams R F, in *Global Analysis* (Proc. of Symp. in Pure Math., Vol. 14, Eds S-S Chern, S Smale) (Providence: Am. Math. Soc., 1970) p. 341
45. Plykin R V *Usp. Mat. Nauk* **35** 94 (1980) [*Russ. Math. Surv.* **35** 109 (1980)]
46. Afraĭmovich V S, Bykov V V, Shil'nikov L P *Dokl. Akad. Nauk SSSR* **234** 336 (1977) [*Sov. Phys. Dokl.* **22** 253 (1977)]
47. Shil'nikov A L, in *Metody Kachestvennoĭ Teorii i Teorii Bifurkatsiĭ* (Methods of Qualitative Theory and Bifurcation Theory) (Ed. L P Shil'nikov) (Gor'kiĭ: Izd. GGU, 1989) p. 130
48. Lozi R *J. Phys. Colloq.* (Paris) **39** (C5) 9 (1978)
49. Belykh V N *Mat. Sbornik* **186** (3) 3 (1995) [*Sbornik Math.* **186** 311 (1995)]
50. Banerjee S, Yorke J A, Grebogi C *Phys. Rev. Lett.* **80** 3049 (1998)
51. Anishchenko V S et al. *Discrete Dyn. Nat. Soc.* **2** 249 (1998)
52. Lai Y-C, Grebogi C, Kurths J *Phys. Rev. E* **59** 2907 (1999)
53. Lai Y-C, Grebogi C *Phys. Rev. Lett.* **82** 4803 (1999)
54. Ott E *Chaos in Dynamical Systems* (Cambridge: Cambridge Univ. Press, 1993)
55. Dawson S et al. *Phys. Rev. Lett.* **73** 1927 (1994)
56. Dawson S P *Phys. Rev. Lett.* **76** 4348 (1996); Moresco P, Dawson S P *Phys. Rev. E* **55** 5350 (1997)
57. Kostelich E J et al. *Physica D* **109** 81 (1997)
58. Lai Y-C et al. *Nonlinearity* **6** 779 (1993)
59. Anishchenko V S et al. *Phys. Lett. A* **270** 301 (2000)
60. Madan R N (Ed.) *Chua's Circuit*: *A Paradigm for Chaos* (Singapore: World Scientific, 1993)
61. Gavrilov N K, Shil'nikov L P *Mat. Sbornik* **88** 475 (1972); **90** 139 (1973)
62. Stratonovich R L, in *Noise in Nonlinear Dynamical Systems* Vol. 2 *Theory of Noise Induced Processes in Special Applications* (Eds F Moss, P V E McClintock) (Cambridge: Cambridge Univ. Press, 1989) p. 16
63. Horsthemke W, Lefever R *Noise-Induced Transitions* (Berlin: Springer-Verlag, 1984)
64. Gardiner C W *Handbook of Stochastic Methods for Physics, Chemistry, and the Natural Sciences* (Berlin: Springer-Verlag, 1983)
65. Haken H *Advanced Synergetics* (Berlin: Springer-Verlag, 1983)
66. Graham R, in *Noise in Nonlinear Dynamical Systems* Vol. 1 *Theory of Continuous Fokker–Planck Systems* (Eds F Moss, P V E McClintock) (Cambridge: Cambridge Univ. Press, 1988)
67. Anishchenko V S, Ebeling W *Z. Phys. B* **81** 445 (1990)
68. Guckenheimer J *Nature* **298** 358 (1982)
69. Hsu C S, Kim M C *J. Stat. Phys.* **38** 735 (1985)
70. Sinaĭ Ya G *Usp. Mat. Nauk* **46** 147 (1991) [*Russ. Math. Surv.* **46** 177 (1991)]
71. Anishchenko V S, Neĭman A B *Pis'ma Zh. Tekh. Fiz.* **17** (14) 43 (1991) [*Sov. Tech. Phys. Lett.* **17** 510 (1991)]
72. Anishchenko V S, Neiman A B, in *Nonlinear Dynamics of Structures*: *Intern. Symp. on Generation of Large-Scale Structures in Continuous Media, Perm–Moscow, USSR, 11–20 June 1990* (Eds R Z Sagdeev et al.) (Singapore: World Scientific, 1991) p. 21
73. Alonso D et al. *Phys. Rev. E* **54** 2474 (1996)
74. Anishchenko V S et al. *Nonlinear Dynamics of Chaotic and Stochastic Systems* (Berlin: Springer, 2002)
75. Farmer J D *Phys. Rev. Lett.* **47** 179 (1981)
76. Arneodo A, Coullet P, Tresser C *Commun. Math. Phys.* **79** 573 (1981)
77. Rosenblum M G, Pikovsky A S, Kurths J *Phys. Rev. Lett.* **76** 1804 (1996)
78. Stratonovich R L *Topics in the Theory of Random Noise* Vol. 1, 2 (New York: Gordon and Breach, 1963, 1967)
79. Malakhov A N *Fluktuatsii v Avtokolebatel'nykh Sistemakh* (Fluctuations in Self-Oscillatory Systems) (Moscow: Nauka, 1968)
80. Rytov S M *Vvedenie v Statisticheskuyu Radiofiziku* (Introduction to Statistical Radiophysics) (Moscow: Nauka, 1966) [Translated into English: Rytov S M, Kravtsov Yu A, Tatarskii V I *Principles of Statistical Radiophysics* 2nd ed. (Berlin: Springer-Verlag, 1987–1989)]
81. Tikhonov V I, Mironov M A *Markovskie Protsessy* (Markovian Processes) (Moscow: Sov. Radio, 1977)
82. Jackson E A *Perspectives of Nonlinear Dynamics* Vol. 1, 2 (Cambridge: Cambridge Univ. Press, 1989, 1990)
83. Gollub J P, Benson S V *J. Fluid Mech.* **100** 449 (1980); Lesieur M *Turbulence in Fluids*: *Stochastic and Numerical Modelling* (Dordrecht: M. Nijhoff, 1987); Sato S, Sano M, Sawada Y *Phys. Rev. A* **37** 1679 (1988); Kida S, Yamada M, Ohkitani K *Physica D* **37** 116 (1989); Bohr T et al. *Dynamical Systems Approach to Turbulence* (Cambridge Nonlinear Sci. Ser., Vol. 8) (Cambridge: Cambridge Univ. Press, 1998); Aranson I S, Kramer L *Rev. Mod. Phys.* **74** 99 (2002)
84. Kuramoto Y *Chemical Oscillations, Waves, and Turbulence* (Berlin: Springer-Verlag, 1984); Pomeau Y, Manneville P *J. Phys. Lett.* (Paris) **40** 609 (1979); Chaté H, Manneville P *Phys. Rev. Lett.* **58** 112 (1987); Coullet P, Gil L, Lega J *Physica D* **37** 91 (1989); Chaté H *Nonlinearity* **7** 185 (1994)

85. Manneville P, Chaté H *Physica D* **96** 30 (1996); Grinstein G, Jayaprakash C, Pandit R *Physica D* **90** 96 (1996)
86. Ermentrout G B, Kopell N *SIAM J. Math. Anal.* **15** 215 (1984); Yamaguchi Y, Shimizu H *Physica D* **11** 212 (1984); Strogatz S H, Mirollo R E *Physica D* **31** 143 (1988)
87. Osipov G V, Sushchik M M *Phys. Rev. E* **58** 7198 (1998)
88. Ermentrout G B, Troy W C *SIAM J. Appl. Math.* **46** 359 (1986)
89. Akopov A A et al. *Pis'ma Zh. Tekh. Fiz.* **29** (15) 29 (2003) [*Tech. Phys. Lett.* **29** 629 (2003)]
90. Samarskiĭ A A, Gulin A V *Chislennye Metody* (Numerical Techniques) (Moscow: Nauka, 1989)
91. Wolf A et al. *Physica D* **16** 285 (1985)
92. Anishchenko V S et al. *Phys. Rev. E* **69** 036215 (2004)